www.sciencemag.org/cgi/content/341/6147/774/DC1

Supplementary Materials for

Incision into the Eastern Andean Plateau During Pliocene Cooling

Richard O. Lease* and Todd A. Ehlers

*Corresponding author. E-mail: rlease@usgs.gov

Published 16 August 2013, *Science* **341**, 774 (2013)
DOI: 10.1126/science.1239132

This PDF file includes:

Materials and Methods

Laboratory Methods

U-Th/He thermochronometry was performed on euhedral, inclusion-free mineral grains with widths >80 μm. Single crystals were loaded into Nb tubes, degassed with a 960 nm diode laser, and ^{4}He abundances were measured via ^{3}He dilution using a Patterson Instruments quadropole mass spectrometer at the University of Tübingen. U, Th, and Sm concentrations were then measured via isotope dilution using an Element2 inductively coupled plasma mass spectrometer at the University of Arizona. Raw ages were corrected for alpha ejection. Means ages (Table S1) were calculated typically from 4 single-grain analyses (Tables S2-S3). Age uncertainties are reported as the 2σ standard error of replicate analyses for individual samples.

Time-Temperature Modeling

Thermal histories were constructed from inverse modeling performed in the HeFTy software version 1.8.0 (*14*). Kinetic models used are from ref. (*39*) for AHe and ref. (*40*) for ZHe. Input data include the AHe and ZHe ages, grain dimensions, and Uranium and Thorium concentrations (Tables S2-S3). Where available, BAr data was included as a constraint defined by the BAr age ± 2σ and 340-360°C. The model starting point was 50 My older and 150°C hotter than the highest closure temperature thermochronometer analyzed to ensure an initial condition where no daughter products are retained. The model ending point was the mean annual temperature +/-2.5°C. No other model constraints were imposed. HeFTy inverse model settings include: monotonic consistent cooling, paths halved 4 times, episodic randomizer, and no maximum cooling rate. Inversions were run until 50 "good" fits (*14*) were obtained and we report the weighted mean cooling paths in Fig. 3C. Model ages computed based on the weighted mean cooling path match the observed ages either exactly or within 0.3 Ma, a result better than model ages computed from the "best" individual modeled path. Full thermal model results are reported in Fig. S3.

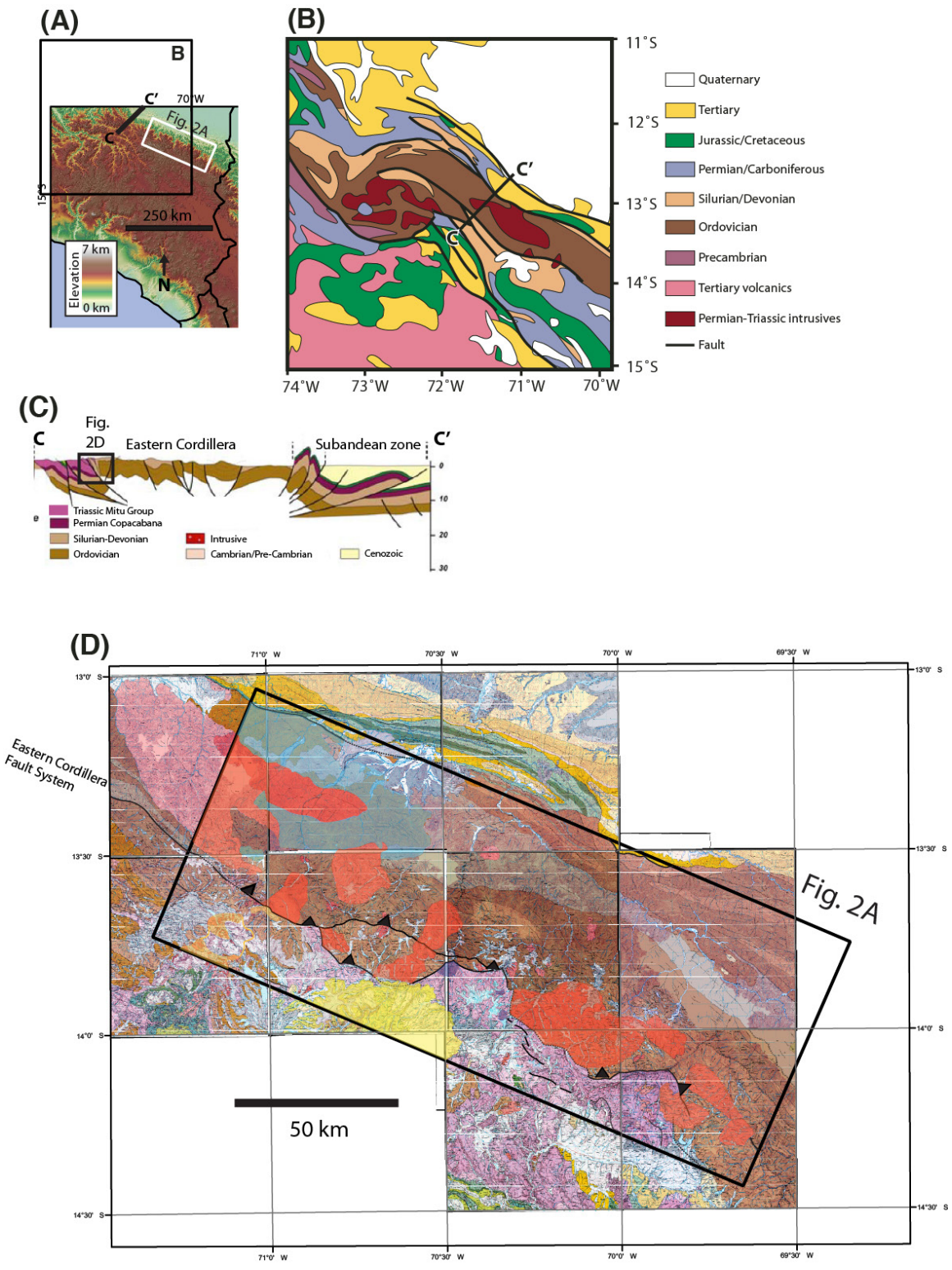

Fig. S1.

Geology of the northeastern Andean Plateau margin. **(A)** Location map. **(B)** General geologic map (*8*). **(C)** Structural cross-section C-C' (*7*). **(D)** Detailed geologic map based on 1:100,000 mapping (*41*).

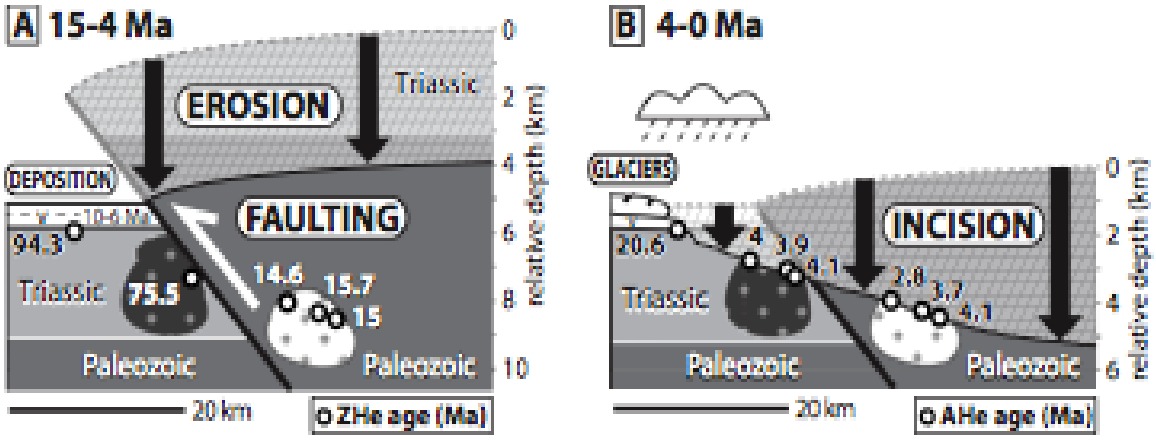

Fig. S2

Schematic cross section depicting evolution of the northeastern Andean Plateau margin since 15 Ma. See Fig. 2 for location.

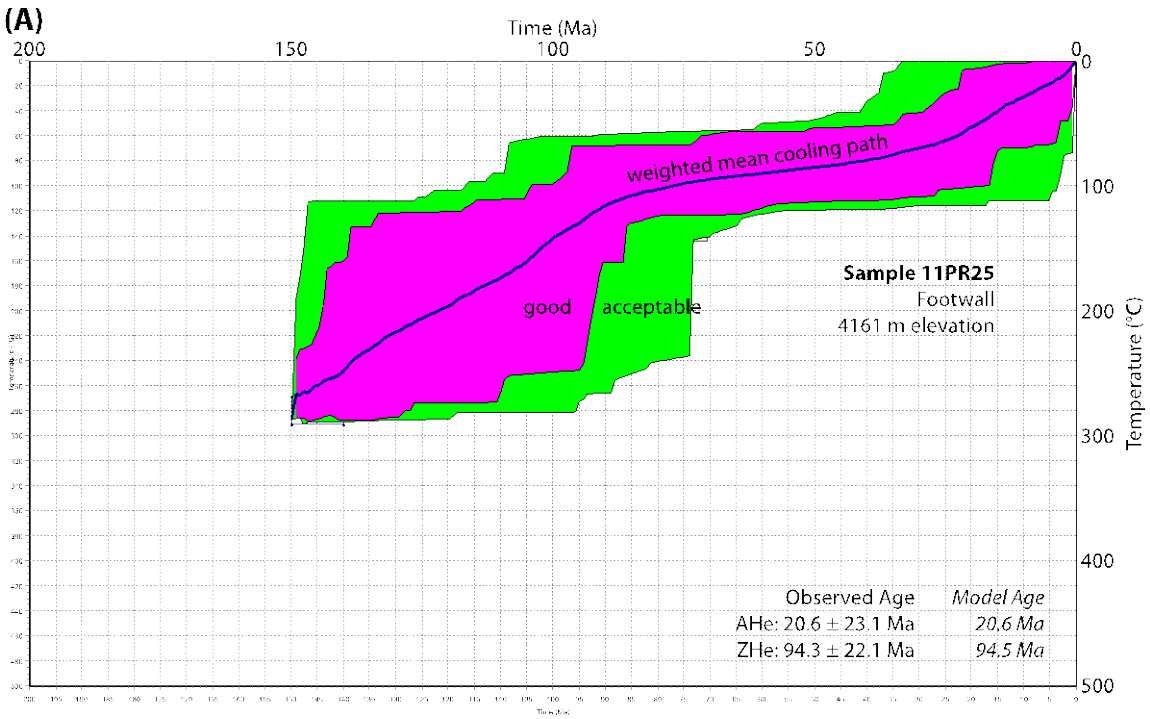
(A)
Time (Ma)
200
150
100
50
0
0
100
200
300
400
500
Temperature (°C)
weighted mean cooling path
good
acceptable
Sample 11PR25
Footwall
4161 m elevation
Observed Age
Model Age
AHe: 20.6 ± 23.1 Ma
20.6 Ma
ZHe: 94.3 ± 22.1 Ma
94.5 Ma

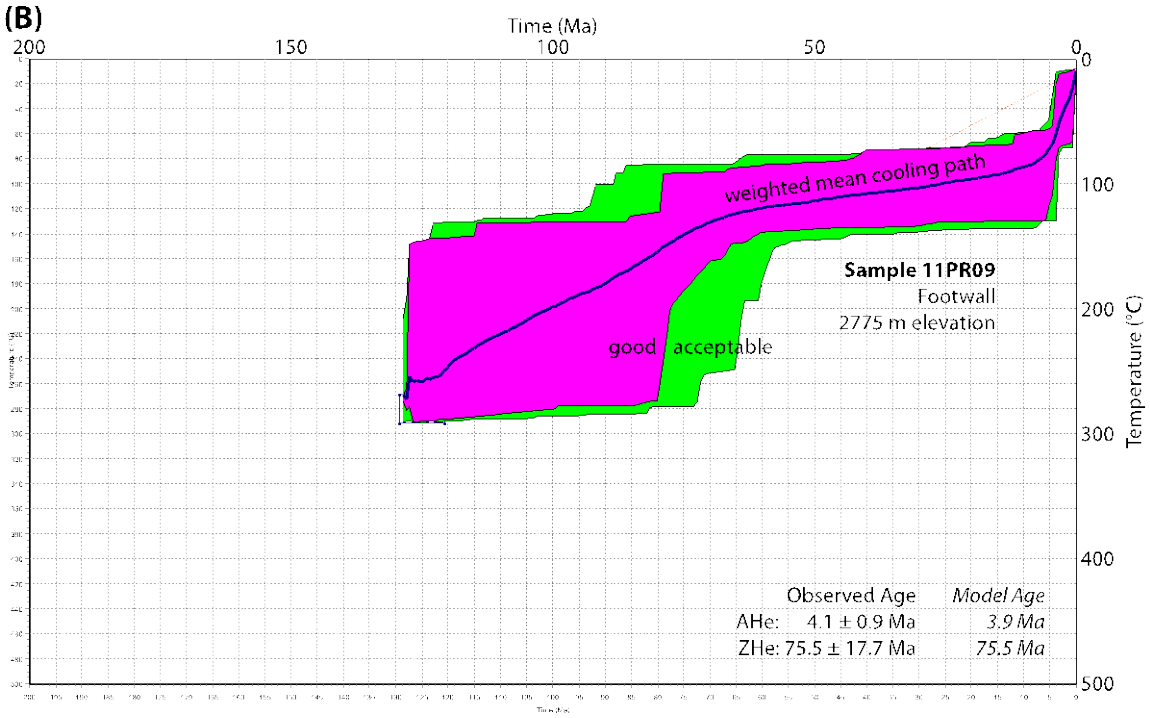
(B)
Time (Ma)
200
150
100
50
0
0
100
200
300
400
500
Temperature (°C)
weighted mean cooling path
good
acceptable
Sample 11PR09
Footwall
2775 m elevation
Observed Age
Model Age
AHe: 4.1 ± 0.9 Ma
3.9 Ma
ZHe: 75.5 ± 17.7 Ma
75.5 Ma

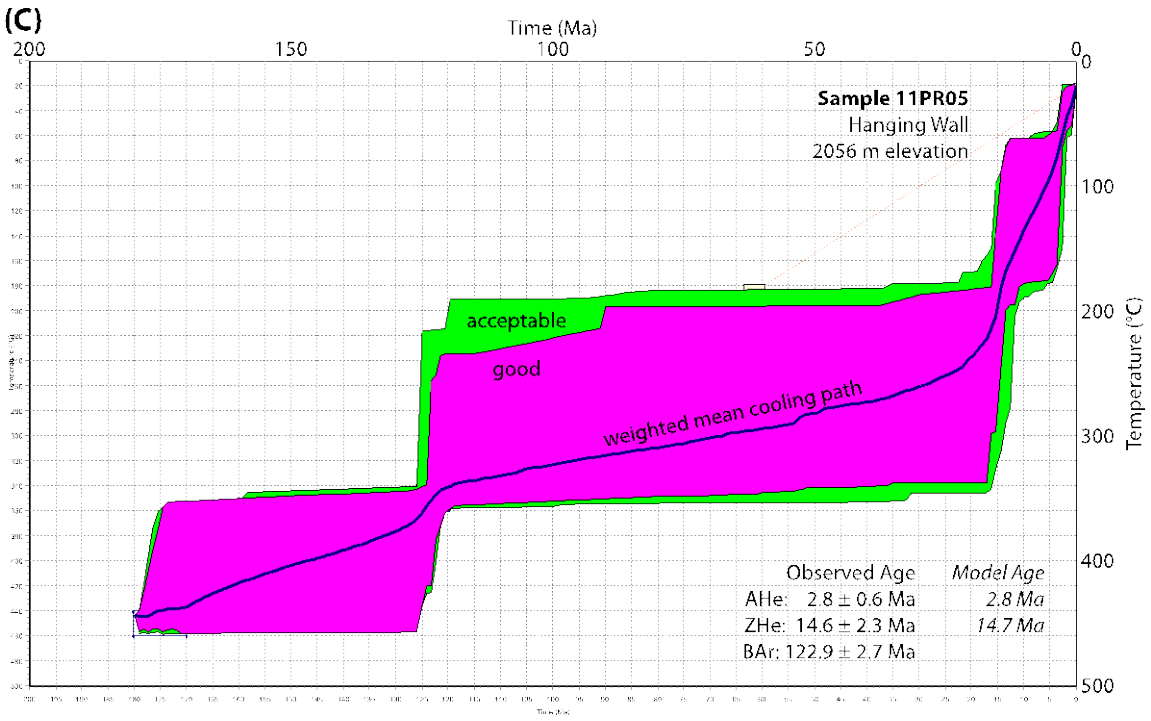
(C)
Time (Ma)
200
150
100
50
0
Sample 11PR05
Hanging Wall
2056 m elevation
acceptable
good
weighted mean cooling path
Observed Age
Model Age
AHe: 2.8 ± 0.6 Ma
2.8 Ma
ZHe: 14.6 ± 2.3 Ma
14.7 Ma
BAr: 122.9 ± 2.7 Ma
Temperature (°C)
0
100
200
300
400
500

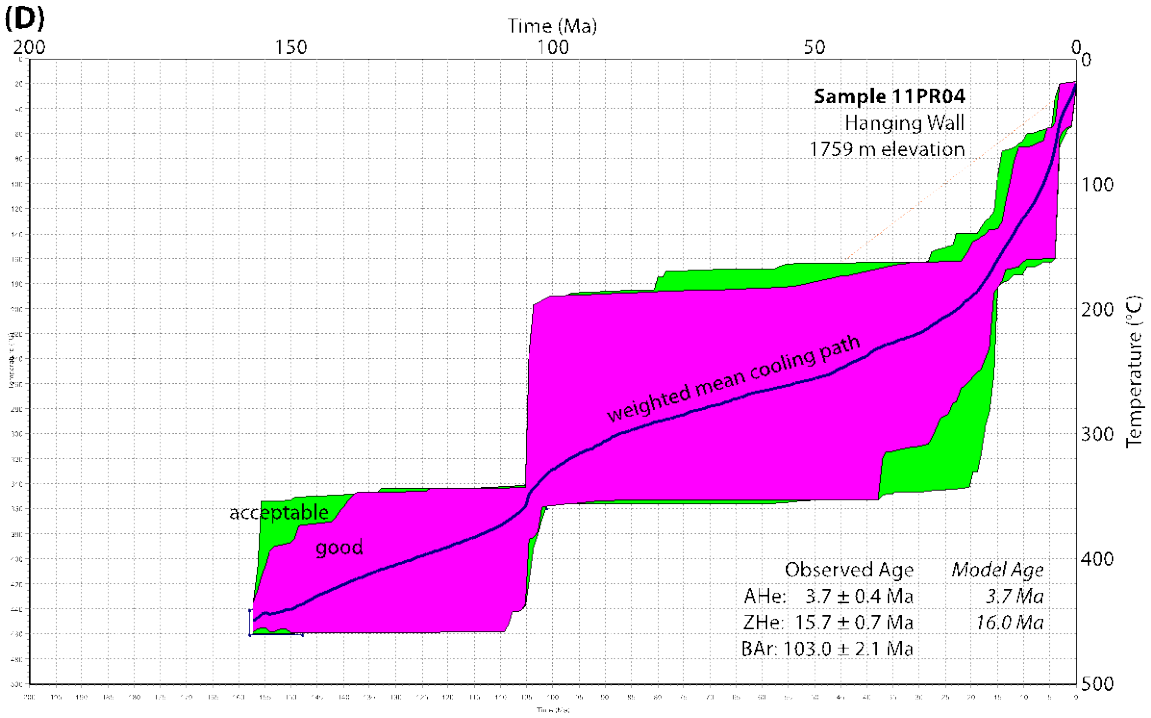
(D)
Time (Ma)
200
150
100
50
0
Sample 11PR04
Hanging Wall
1759 m elevation
acceptable
good
weighted mean cooling path
Observed Age
Model Age
AHe: 3.7 ± 0.4 Ma
3.7 Ma
ZHe: 15.7 ± 0.7 Ma
16.0 Ma
BAr: 103.0 ± 2.1 Ma
Temperature (°C)
0
100
200
300
400
500

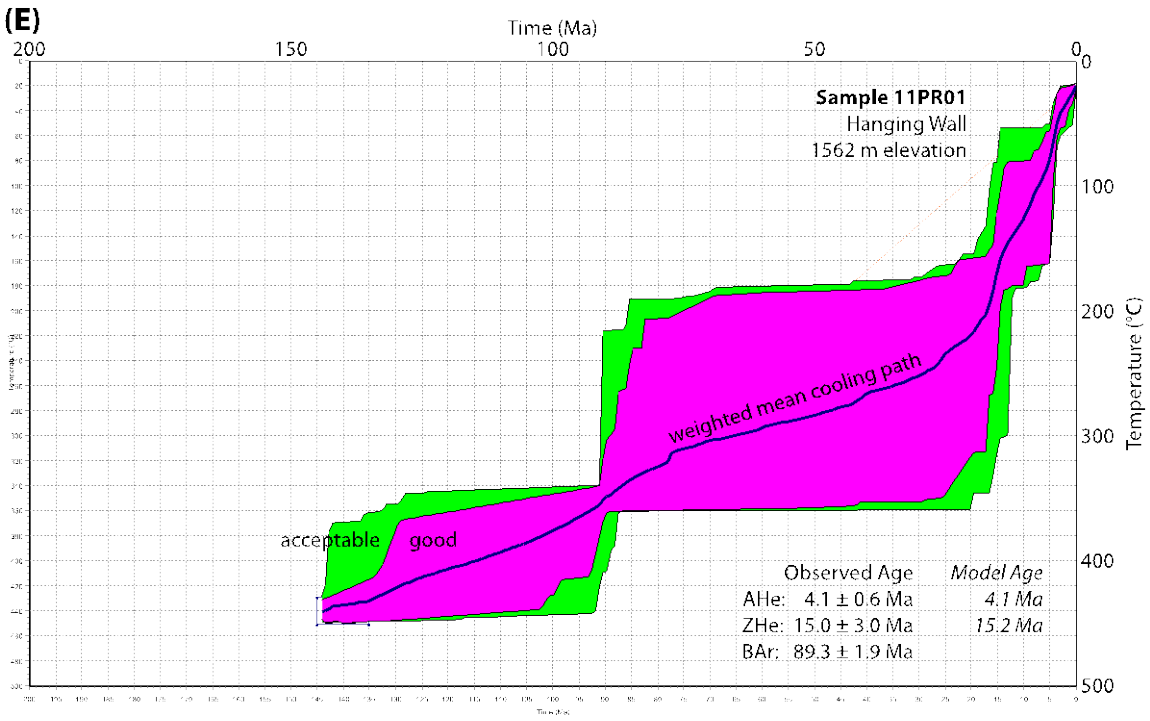

Fig. S3

Results from inverse time-temperature modeling with the HeFTy software. Samples **(A)** 11PR25, **(B)** 11PR09, **(C)** 11PR05, **(D)** 11PR04, **(E)** 11PR01. Model age computed from weighted mean cooling path.

Table S1.
Apatite (U-Th)/He, zircon (U-Th)/He, and biotite K/Ar ages.

Sample	latitude	longitude	elevation (m)	AHe mean age (Ma)	error (2σ)	ZHe mean age (Ma)	error (2σ)	BAr age (Ma)*	error (2σ)*	incision depth (km)
11PR01	-13.650	-70.474	1562	4.1	0.6	15.0	3	89.3	1.9	2.38
11PR04	-13.667	-70.478	1759	3.7	0.4	15.7	0.7	103.0	2.1	2.25
11PR05	-13.711	-70.455	2056	2.8	0.6	14.6	2.3	122.9	2.7	2.29
11PR09	-13.807	-70.479	2775	4.1	0.9	75.5**	17.7**			2.08
11PR11	-13.808	-70.475	2974	3.9	1.9					1.90
11PR16	-13.847	-70.504	3240	4.0	0.2					1.91
11PR25	-13.929	-70.499	4161	20.6	23.1	94.3	22.1			0.50

Notes:

* BAr ages from ref. (*13*). Our sample 11PR01 correlates to sample COCA-343B of ref. (*13*), 11PR04 to COCA-344, and 11PR05 to COCA-346

** Single replicate age. 23% error assumed from adjacent sample 11PR25.

Table S2.

Single grain apatite (U-Th)/He analyses.

Sample	4-He (mol)	238-U (mol)	235-U (mol)	232-Th (mol)	147-Sm (mol)	Raw Age (Ma)	Ft #	Corr Age (Ma)
11PR01_1	9.51E-16	2.63E-13	1.95E-15	1.24E-13	3.96E-13	2.51	0.69	3.65
11PR01_2	1.38E-15	2.81E-13	2.08E-15	1.91E-13	7.00E-13	3.26	0.73	4.45
11PR01_3	1.09E-15	1.99E-13	1.47E-15	2.30E-13	7.16E-13	3.33	0.71	4.71
11PR01_4	1.64E-15	4.56E-13	3.37E-15	1.01E-13	6.68E-13	2.63	0.73	3.62
11PR04_1	1.22E-14	2.68E-12	1.98E-14	3.62E-13	2.21E-12	3.40	0.83	4.08
11PR04_2	6.90E-15	1.86E-12	1.37E-14	4.82E-13	1.51E-12	2.70	0.82	3.30
11PR04_3	5.26E-15	1.34E-12	9.91E-15	1.73E-13	1.11E-12	2.94	0.75	3.95
11PR04_4	2.61E-15	7.64E-13	5.65E-15	1.58E-13	7.42E-13	2.51	0.76	3.29
11PR05_2	1.52E-15	3.94E-13	2.91E-15	5.55E-14	4.55E-13	2.87	0.75	3.81
11PR05_3	1.13E-15	3.76E-13	2.78E-15	1.85E-13	4.70E-13	2.08	0.70	2.96
11PR05_4	3.39E-16	1.89E-13	1.39E-15	4.66E-14	2.38E-13	1.31	0.73	1.80
11PR05_5	1.55E-15	5.68E-13	4.20E-15	7.46E-14	5.55E-13	2.05	0.75	2.71
11PR05_6	1.20E-15	4.50E-13	3.33E-15	6.78E-14	3.29E-13	1.99	0.71	2.81
11PR11_1	1.56E-15	3.26E-13	2.41E-15	1.46E-12	1.07E-12	1.82	0.73	2.50
11PR11_2	3.85E-15	2.85E-13	2.11E-15	1.14E-12	9.60E-13	5.42	0.71	7.62
11PR11_3	3.98E-15	3.32E-13	2.46E-15	1.24E-12	9.83E-13	4.97	0.73	6.84
11PR11_4	3.67E-16	2.48E-13	1.83E-15	9.29E-13	6.55E-13	0.61	0.66	0.93
11PR11_5	1.12E-15	2.19E-13	1.62E-15	6.21E-13	5.43E-13	2.39	0.72	3.30
11PR11_6	1.75E-15	2.93E-13	2.17E-15	8.53E-13	6.81E-13	2.77	0.69	4.02
11PR11_7	1.49E-15	6.56E-13	4.85E-15	5.53E-13	4.75E-13	1.47	0.67	2.21
11PR16_1	1.89E-15	5.10E-13	3.77E-15	6.45E-14	4.65E-13	2.78	0.69	4.02
11PR16_2	1.92E-15	5.39E-13	3.99E-15	2.77E-14	4.44E-13	2.72	0.66	4.11
11PR16_3	2.54E-15	7.30E-13	5.40E-15	6.64E-14	5.02E-13	2.63	0.69	3.82
11PR09_1	5.07E-15	6.55E-13	4.85E-15	1.87E-12	2.02E-12	3.60	0.77	4.69
11PR09_2	2.05E-15	2.94E-13	2.17E-15	1.01E-12	9.69E-13	3.01	0.69	4.37
11PR09_3*	7.66E-16	6.11E-13	4.52E-15	6.18E-13	6.56E-13	0.79	0.67	1.17
11PR09_4	3.48E-15	7.54E-13	5.58E-15	1.56E-12	1.45E-12	2.42	0.74	3.25
11PR25_1	2.61E-15	1.54E-13	1.14E-15	1.59E-13	5.13E-14	10.6	0.67	15.8
11PR25_2	2.80E-15	8.88E-13	6.57E-15	6.43E-14	6.19E-13	2.40	0.73	3.31
11PR25_3	2.92E-16	7.87E-15	5.82E-17	1.72E-15	1.78E-13	24.6	0.58	42.5

Notes:

* Anomalously young age. Replicate age is >70% younger than the mean of the other three replicates and shows insufficient helium compared to other replicates with similar U and Th values. This may be due to partial degassing. Age excluded from the calculation of the mean and standard deviation.

Ft is alpha-correction after ref. (*42*)

Table S3.

Single grain zircon (U-Th)/He analyses.

Sample	4-He (mol)	238-U (mol)	235-U (mol)	232-Th (mol)	Raw Age (Ma)	Ft #	Corr Age (Ma)
11PR01Z-1	9.26E-13	5.10E-11	3.77E-13	2.16E-11	12.80	0.859	14.9
11PR01Z-2	3.58E-13	2.38E-11	1.76E-13	1.09E-11	10.52	0.842	12.5
11PR01Z-3	4.97E-13	2.27E-11	1.68E-13	1.55E-11	14.62	0.826	17.7
11PR04Z-1	2.31E-13	1.20E-11	8.87E-14	7.66E-12	12.99	0.812	16.0
11PR04Z-2	2.48E-13	1.38E-11	1.02E-13	9.44E-12	12.03	0.805	14.9
11PR04Z-3	1.82E-13	9.65E-12	7.14E-14	5.73E-12	12.83	0.799	16.1
11PR05Z-1	9.17E-13	6.43E-11	4.76E-13	1.80E-11	10.37	0.814	12.7
11PR05Z-2	8.29E-13	5.00E-11	3.70E-13	1.97E-11	11.77	0.812	14.5
11PR05Z-3	1.22E-12	6.49E-11	4.80E-13	2.25E-11	13.51	0.812	16.6
11PR09Z-2	2.26E-13	2.78E-12	2.06E-14	1.78E-12	54.72	0.723	75.5
11PR25Z-1	3.21E-13	3.21E-12	2.38E-14	3.54E-12	61.53	0.843	72.9
11PR25Z-2	2.69E-13	1.96E-12	1.45E-14	2.32E-12	83.11	0.832	99.8
11PR25Z-3	2.66E-13	1.80E-12	1.33E-14	2.19E-12	88.87	0.806	110.1

Notes:

Ft is alpha-correction after ref. (*42*)

References

1. T. F. Schildgen, K. V. Hodges, K. X. Whipple, P. W. Reiners, M. S. Pringle, Uplift of the western margin of the Andean plateau revealed from canyon incision history, southern Peru. *Geology* **35**, 523–526 (2007). doi:10.1130/G23532A.1

2. G. D. Hoke, B. L. Isacks, T. E. Jordan, N. Blanco, A. J. Tomlinson, J. Ramezani, Geomorphic evidence for post-10 Ma uplift of the western flank of the central Andes 18°30′-22°S. *Tectonics* **26**, TC5021 (2007). doi:10.1029/2006TC002082

3. C. N. Garzione, G. D. Hoke, J. C. Libarkin, S. Withers, B. MacFadden, J. Eiler, P. Ghosh, A. Mulch, Rise of the Andes. *Science* **320**, 1304–1307 (2008). doi:10.1126/science.1148615 Medline

4. T. A. Ehlers, C. J. Poulsen, Influence of Andean uplift on climate and paleoaltimetry estimates. *Earth Planet. Sci. Lett.* **281**, 238–248 (2009). doi:10.1016/j.epsl.2009.02.026

5. L. Kennan, S. H. Lamb, L. Hoke, High-altitude palaeosurfaces in the Bolivian Andes: Evidence for late Cenozoic surface uplift. *Geol. Soc. Lond. Spec. Publ.* **120**, 307–323 (1997). doi:10.1144/GSL.SP.1997.120.01.20

6. G. Zeilinger, F. Schlunegger, Possible flexural accommodation on the eastern edge of the Altiplano in relation to focussed erosion in the Rio La Paz drainage system. *Terra Nova* **19**, 373–380 (2007). doi:10.1111/j.1365-3121.2007.00762.x

7. V. Carlotto, *Bol. Soc. Geol. Peru* **101**, 91–119 (2006).

8. N. Gotberg, N. McQuarrie, V. C. Caillaux, Comparison of crustal thickening budget and shortening estimates in southern Peru (12-14 S): Implications for mass balance and rotations in the “Bolivian orocline”. *Geol. Soc. Am. Bull.* **122**, 727–742 (2010). doi:10.1130/B26477.1

9. A. Cheilletz, A. H. Clark, E. Farrar, G. A. Pauca, M. Pichavant, H. A. Sandeman, Volcano-stratigraphy and 40Ar/39Ar geochronology of the Macusani ignimbrite field: Monitor of the Miocene geodynamic evolution of the Andes of southeast Peru. *Tectonophysics* **205**, 307–327 (1992). doi:10.1016/0040-1951(92)90433-7

10. L. G. Thompson, E. Mosley-Thompson, B. M. Arnao, El Nino-Southern Oscillation events recorded in the stratigraphy of the tropical Quelccaya ice cap, Peru. *Science* **226**, 50–53 (1984). doi:10.1126/science.226.4670.50 Medline

11. A. G. Klein, G. O. Seltzer, B. L. Isacks, Modern and last local glacial maximum snowlines in the Central Andes of Peru, Bolivia, and Northern Chile. *Quat. Sci. Rev.* **18**, 63–84 (1999). doi:10.1016/S0277-3791(98)00095-X

12. P. W. Reiners, M. T. Brandon, Using thermochronology to understand orogenic erosion. *Annu. Rev. Earth Planet. Sci.* **34**, 419–466 (2006). doi:10.1146/annurev.earth.34.031405.125202

13. D. J. Kontak, E. Farrar, A. H. Clark, D. A. Archibald, Eocene tectono-thermal rejuvenation of an upper Paleozoic-lower Mesozoic terrane in the Cordillera de Carabaya, Puno, southeastern Peru, revealed by K-Ar and $^{40}Ar/^{39}Ar$ dating. *J. S. Am. Earth Sci.* **3**, 231–246 (1990). doi:10.1016/0895-9811(90)90005-L

14. R. A. Ketcham, Forward and inverse modeling of low-temperature thermochronometry data. *Rev. Mineral.* **58**, 275–314 (2005). doi:10.2138/rmg.2005.58.11

15. T. F. Schildgen, G. Balco, D. L. Shuster, Canyon incision and knickpoint propagation recorded by apatite $^{4}He/^{3}He$ thermochronometry. *Earth Planet. Sci. Lett.* **293**, 377–387 (2010). doi:10.1016/j.epsl.2010.03.009

16. N. McQuarrie, J. B. Barnes, T. A. Ehlers, Geometric, kinematic, and erosional history of the central Andean Plateau, Bolivia (15-17°S). *Tectonics* **27**, TC3007 (2008). doi:10.1029/2006TC002054

17. J. B. Barnes, T. A. Ehlers, N. Insel, N. McQuarrie, C. J. Poulsen, Linking orography, climate, and exhumation across the central Andes. *Geology* **40**, 1135–1138 (2012). doi:10.1130/G33229.1

18. B. K. Horton, Revised deformation history of the central Andes: Inferences from Cenozoic foredeep and intermontane basins of the Eastern Cordillera, Bolivia. *Tectonics* **24**, TC3011 (2005). doi:10.1029/2003TC001619

19. S. L. Beck, G. Zandt, The nature of orogenic crust in the central Andes. *J. Geophys. Res.* **107**, (B10), 2230 (2002). doi:10.1029/2000JB000124

20. C. Hoorn, F. P. Wesselingh, H. ter Steege, M. A. Bermudez, A. Mora, J. Sevink, I. Sanmartín, A. Sanchez-Meseguer, C. L. Anderson, J. P. Figueiredo, C. Jaramillo, D. Riff, F. R. Negri, H. Hooghiemstra, J. Lundberg, T. Stadler, T. Särkinen, A. Antonelli, Amazonia through time: Andean uplift, climate change, landscape evolution, and biodiversity. *Science* **330**, 927–931 (2010). doi:10.1126/science.1194585 Medline

21. A. V. Fedorov, C. M. Brierley, K. T. Lawrence, Z. Liu, P. S. Dekens, A. C. Ravelo, Patterns and mechanisms of early Pliocene warmth. *Nature* **496**, 43–49 (2013). doi:10.1038/nature12003 Medline

22. A. V. Fedorov, P. S. Dekens, M. McCarthy, A. C. Ravelo, P. B. deMenocal, M. Barreiro, R. C. Pacanowski, S. G. Philander, The Pliocene paradox (mechanisms for a permanent El Niño). *Science* **312**, 1485–1489 (2006). doi:10.1126/science.1122666 Medline

23. R. Garreaud, M. Vuille, A. C. Clement, The climate of the Altiplano: Observed current conditions and mechanisms of past changes. *Palaeogeogr. Palaeoclimatol. Palaeoecol.* **194**, 5–22 (2003). doi:10.1016/S0031-0182(03)00269-4

24. M. Mudelsee, M. E. Raymo, Slow dynamics of the Northern Hemisphere glaciation. *Paleoceanography* **20**, PA4022 (2005). doi:10.1029/2005PA001153

25. L. G. Thompson, E. Mosley-Thompson, M. E. Davis, V. S. Zagorodnov, I. M. Howat, V. N. Mikhalenko, P. N. Lin, Annually resolved ice core records of tropical climate variability over the past ~1800 years. *Science* **340**, 945–950 (2013). doi:10.1126/science.1234210 Medline

26. J. C. Chiang, M. Biasutti, D. S. Battisti, Sensitivity of the Atlantic Intertropical Convergence Zone to Last Glacial Maximum boundary conditions. *Paleoceanography* **18**, 1094 (2003). doi:10.1029/2003PA000916

27. P. A. Baker, G. O. Seltzer, S. C. Fritz, R. B. Dunbar, M. J. Grove, P. M. Tapia, S. L. Cross, H. D. Rowe, J. P. Broda, The history of South American tropical precipitation for the past 25,000 years. *Science* **291**, 640–643 (2001). doi:10.1126/science.291.5504.640 Medline

28. C. J. Poulsen, T. A. Ehlers, N. Insel, Onset of convective rainfall during gradual late Miocene rise of the central Andes. *Science* **328**, 490–493 (2010). doi:10.1126/science.1185078 Medline

29. K. L. Ferrier, K. L. Huppert, J. T. Perron, Climatic control of bedrock river incision. *Nature* **496**, 206–209 (2013). doi:10.1038/nature11982 Medline

30. B. Bookhagen, M. R. Strecker, in *Amazonia: Landscape and Species Evolution*, C. Hoorn, F. P. Wesselingh, Eds. (Wiley-Blackwell Publishing Ltd., Oxford, UK, 2010), pp. 223–241.

31. R. Aalto, L. Maurice-Bourgoin, T. Dunne, D. R. Montgomery, C. A. Nittrouer, J. L. Guyot, Episodic sediment accumulation on Amazonian flood plains influenced by El Niño/Southern Oscillation. *Nature* **425**, 493–497 (2003). doi:10.1038/nature02002 Medline

32. R. S. Bradley, M. Vuille, D. Hardy, L. G. Thompson, Low latitude ice cores record Pacific sea surface temperatures. *Geophys. Res. Lett.* **30**, 1174 (2003). doi:10.1029/2002GL016546

33. C. J. Placzek, J. Quade, P. J. Patchett, Geochronology and stratigraphy of late Pleistocene lake cycles on the southern Bolivian Altiplano: Implications for causes of tropical climate change. *Geol. Soc. Am. Bull.* **118**, 515–532 (2006). doi:10.1130/B25770.1

34. L. G. Thompson, M. E. Davis, E. Mosley-Thompson, T. A. Sowers, K. A. Henderson, V. S. Zagorodnov, P. Lin, V. N. Mikhalenko, R. K. Campen, J. F. Bolzan, J. Cole-Dai, B. Francou, A 25,000-year tropical climate history from Bolivian ice cores. *Science* **282**, 1858–1864 (1998). doi:10.1126/science.282.5395.1858 Medline

35. S. C. Fritz, P. A. Baker, G. O. Seltzer, A. Ballantyne, P. Tapia, H. Cheng, R. L. Edwards, Quaternary glaciation and hydrologic variation in the South American tropics as reconstructed from the Lake Titicaca drilling project. *Quat. Res.* **68**, 410–420 (2007). doi:10.1016/j.yqres.2007.07.008

36. C. J. Placzek, J. Quade, P. J. Patchett, A 130 ka reconstruction of rainfall on the Bolivian Altiplano. *Earth Planet. Sci. Lett.* **363**, 97–108 (2013). doi:10.1016/j.epsl.2012.12.017

37. C. M. Clapperton, Glaciation in Bolivia before 3.27 Myr. *Nature* **277**, 375–377 (1979). doi:10.1038/277375a0

38. R. Gaupp, A. Kött, G. Wörner, Palaeoclimatic implications of Mio-Pliocene sedimentation in the high-altitude intra-arc Lauca Basin of northern Chile. *Palaeogeogr. Palaeoclimatol. Palaeoecol.* **151**, 79–100 (1999). doi:10.1016/S0031-0182(99)00017-6

39. R. M. Flowers, R. A. Ketcham, D. L. Shuster, K. A. Farley, Apatite (U-Th)/He thermochronometry using a radiation damage accumulation and annealing model. *Geochim. Cosmochim. Acta* **73**, 2347–2365 (2009). doi:10.1016/j.gca.2009.01.015

40. W. R. Guenthner, P. W. Reiners, R. A. Ketcham, L. Nasdala, G. Giester, Helium diffusion in natural zircon: Radiation damage, anisotropy, and the interpretation of zircon (U-Th)/He thermochronology. *Am. J. Sci.* **313**, 145–198 (2013). doi:10.2475/03.2013.01

41. Peru Geological, Mining, and Metallurgical Institute (Instituto Geológico Minero y Metalurgico), Series A: National Geologic Maps 1:100,000 scale, Maps 27-T, U, V; 28-T, U, V, X; 29-V, X (1999).

42. K. A. Farley, R. A. Wolf, L. T. Silver, The effects of long alpha-stopping distances on (U-Th)/He ages. *Geochim. Cosmochim. Acta* **60**, 4223–4229 (1996). doi:10.1016/S0016-7037(96)00193-7